Pergamon

Spectrochimica Acta, Vol. 51A, No. 6, pp. 1061–1074, 1995

0584–8539(94)00114–P
0584–8539/95 $9.50 + 0.00

Vibrational assignments of 3-alkyl-3,4-dihydro-6-methyl-2H-1,3-benzoxazines in the fingerprint region

J. DUNKERS† and H. ISHIDA

Department of Macromolecular Science, Case Western Reserve University, Cleveland, OH 44106, U.S.A.

(*Received* 29 *October* 1993; *in final form and accepted* 5 *April* 1994)

Abstract—Fundamental vibrational assignments of a series of 3-alkyl-3,4-dihydro-6-methyl-2H-1,3-benzoxazines are made by analysis of the fingerprint region (2000–500 cm^{-1}) of their infrared and Raman spectra. The linear amine group is varied from methyl to amyl which alters the position of the peaks resulting from the oxazine ring but has little influence on the benzene ring vibrations. To aid in the peak assignments, 3,4-dideutero-3,6-dimethyl-2D-1,3-benzoxazine has also been synthesized. The structures of the compounds are verified by ^{1}H and ^{13}C NMR.

INTRODUCTION

BENZOXAZINE based phenolic resins attempt to solve the shortcomings associated with traditional phenolic resins. Resole and novolac resins suffer from evolution of volatiles upon curing, strong catalysts, and a poor shelf life. Benzoxazine curing is a ring opening reaction initiated by a molecule with an active proton which eliminates the problem of volatiles. Also, catalysts weaker than those employed with conventional phenolics are used for curing. Holly and Cope [1] were the first to propose the 3,4-dihydro-2H-1,3-benzoxazine structure from the condensation of formaldehyde with *o*-hydroxybenzylamine in 1944. Burke [2] was the first to seriously investigate the Mannich condensation of phenols, formaldehyde, and primary amines in the ratio of 1:2:1 in dioxane. The formation of benzoxazine proceeds according to Scheme 1. The yields of benzoxazine were influenced by the primary amine and the nature of the substituent on the benzene ring *para* to the oxygen atom. The results showed that the presence of an electron withdrawing substituent at either site decreased the yield of benzoxazine. The addition of chlorine and bromine atoms at the *ortho* and *para* sites on the benzene ring had less of an influence on the yield than the electronegativity and steric hindrance of the amine [3]. In one of Burke's later papers, purified benzoxazines were converted to dimers upon addition of 2-methyl or 2,5-dimethyl phenol [4]. It was found that the aminoalkylation occurred preferentially at the free *ortho* position. From his experiments, the benzoxazines derived from methyl amines were found to be more reactive than those from the aniline while the cyclohexyl substituent had intermediate reactivity.

In a more detailed work by Riess *et al.* [5], the kinetics of ring opening dimerization were studied using ^{1}H nuclear magnetic resonance (NMR) spectroscopy and size exclusion chromatography (SEC). From activiation energy calculations, the energy for ring opening of benzoxazine was the smallest for dimerization using dimethyl phenol and increased substantially with 2,4-ditertbutyl phenol. In addition, there have been a number of papers that have investigated the conformation of 2,4-alkyl substituted benzoxazines using ^{1}H and ^{13}C NMR spectroscopy [6, 7]. In the most recent work on benzoxazines, Ning and Ishida synthesized bifunctional benoxazines to overcome the low degree of cure associated with monofunctional systems [8]. They studied the synthesis and curing of bisphenol-A based benzoxazines using Fourier transform infrared spectroscopy (FT-IR), SEC, ^{1}H NMR and differential scanning calorimetry.

Using the work of Ning and Ishida as a foundation, more detailed studies of benzoxazines as monomers for novel phenolic resins are being pursued. From a molecular perspective, infrared and Raman spectroscopies are very effective in meeting

† Corresponding author: Present address: NIST, Polymers Division, Gaithersburg, MD 20899, U.S.A.

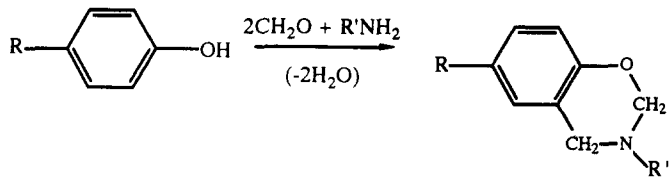

Scheme 1.

these goals. However, the vibrational spectra of these benzoxazines are very complicated and not easily assignable upon first inspection. There is very little information in the literature that can aid in the assignment of the vibrational spectra of these molecules [9, 10]. Therefore, a detailed study of these molecules was needed. The goal of this work was to provide assignments in the fingerprint region that can be used as diagnostic bands to study benzoxazine synthesis and polymerization. In this paper, a systematic set of 3-alkyl-3,4-dihydro-6-methyl-2H-1,3-benzoxazines derived from *p*-cresol, formaldehyde and aliphatic amines were synthesized. The amines were linear ranging from methyl to amyl amine. By changing the weight of the amine attached to the benzoxazine ring, the peaks attributable to the benzoxazine ring varied in position while the modes due to the benzene ring remained stable in position and relative intensity. Using information gathered from infrared and Raman spectra of these model compounds, peaks in the fingerprint region of the spectra were assigned. A complete analysis of the vibrational modes can only be accomplished through normal coordinate analysis since contributions from different modes can be contained in one peak. However, by using information from the literature, by comparing the systematically varied spectra of the benzoxazines, and by analyzing compounds of similar structure, vibrational assignments of the benzoxazine molecule were deduced.

EXPERIMENTAL

All chemicals were used as received. The formaldehyde and amines were purchased from Aldrich. The formaldehyde is 37% by weight in water. The purity of the amines is as follows: methyl (40% in water), ethyl (70% in water), propyl (98%), butyl (98%), amyl (97%). The *p*-cresol was purchased from Fluka chemicals and is 99% + pure. The deuterated formaldehyde was purchased from Cambridge Isotope Labs and is 20 wt.% formaldehyde d-2 in D_2O. The 2,4-dimethylphenol was purchased from Kodak and is 99% pure. For the synthesis of the monofunctional benzoxazine, the mole ratio of amine : formaldehyde : *p*-cresol was 1 : 2 : 1. To synthesize the benzoxazine model compounds, the procedure described below was followed [2]. To 16.2 ml of formaldehyde solution in 80 ml dioxane, 0.1 mol of amine was added dropwise. This mixture was stirred for 10 min in an ice bath. To this mixture, 10.81 g *p*-cresol in 100 ml dioxane was added. This stirring reaction mixture was refluxed for 6 h. After the reactants cooled to room temperature, the dioxane was removed with a rotovap, and the benzoxazine monomer was redissolved into 200 ml ethyl ether. The ether solution was decanted into a separatory funnel and washed four times with a 50 ml portion of 3 N NaOH aqueous solution. After washing, the ether phase was dried over sodium sulfate. The ether phase was again removed with a rotovap. The benzoxazines after evaporation were clear, pale, yellowish liquids at room temperature except for the methyl benzoxazine which was a pale, yellow solid. The liquid benzoxazines were purified with vacuum distillation, while the methyl amine based benzoxazine was purified with vacuum sublimation. The benzoxazine purity was verified using high performance liquid chromatography (HPLC).

The methylene protons of the benzoxazine ring were replaced with deuterium atoms to aid in band assignments. The deuterated benzoxazine was synthesized as follows. To 3.2 g of deuterated formaldehyde solution in 8 ml dioxane, 0.82 ml of methyl amine was added. The mixture was stirred for 10 min in an ice bath. To this mixture, 1.08 g of *p*-cresol was added. The reaction was refluxed for 6 h. The rest of the procedure is identical to the previous description. The deuterated benzoxazine was purified by vacuum sublimation to white crystals.

The infrared spectra were taken on a Michelson 110 MB Fourier transform infrared spectrometer. Three hundred coadded scans were taken at a resolution of 2 cm^{-1} using a liquid nitrogen cooled MCT detector after a 20 min purge with nitrogen. The specific detectivity of the detector,

D^*, was 1×10^{10} cm $Hz^{1/2}$ W^{-1}. All samples were thin films of liquid benzoxazine between two KBr plates.

The Raman spectra were taken on a Dilor XY dispersive spectrometer. The spectrometer was equipped with a triple monochromator having holographic gratings of 1200 grooves mm^{-1}. The detector was an 18 bit charge coupled device. The excitation source was a Coherent Model 890 Ti:Sapphire laser at 750.7 nm pumped by a Coherent Innova Model 305 argon ion laser at multi-line visible. An interference filter with a maximum 61% transmittance at 750.7 nm was inserted into the beam path to eliminate a small amount of background emitted from the Ti:Sapphire laser. The benzoxazines were placed in a capillary bulb, and the bulb was inserted into the macro sample chamber. The spectra were taken using 50–70 mW power measured at the sample. The slit width was 200 μm which resulted in a resolution of 3.4 cm^{-1} at the excitation frequency. The detector integration time was 300 s. Both the IR and Raman spectra of the methyl amine functional benzoxazine were taken of the material in a liquid state at 32°C. The melting point of the methyl benzoxazine crystals is 29°C.

The ^1H NMR spectra were taken on a Varian XL-200 spectrometer. Acetone d-6 was used as a solvent and tetramethylsilane (TMS) was used as a standard. The ^{13}C NMR spectra were acquired on a Varian XL-200 with proton decoupling. Deuterated chloroform was used as a solvent and TMS was an internal standard.

Results and Discussion

Nuclear magnetic resonance spectroscopy

The structure of 3,4-dihydro-6-methoxy-3-methyl-2H-1,3-benzoxazine was verified by single crystal X-ray diffraction [11]. The NMR assignments of the model compounds are confirmed by the work of Proponet *et al.* [12]. The ^1H and ^{13}C NMR spectra of the methyl amine based benzoxazine with hydrogenated and deuterated methylene groups are shown in Figs 1 and 2. The benzoxazine structure along with the peak positions is displayed in Table 1. As expected, the methylene protons present in Fig. 1A from the oxazine ring are absent in the spectrum of the deuterated compound in Fig. 1B. A better confirmation of the benzoxazine structure is the ^{13}C NMR spectra in Fig. 2. In the deuterated benzoxazine spectrum, the intensity of the methylene carbon peaks decreases due to the removal of the nuclear Overhauser effect (NOE), the increase in carbon relaxation time, and the splitting into pentets.

Infrared and Raman assignments

The symmetry of the benzoxazine molecule is C_1 since the nitrogen atom is out of the plane of the benzoxazine ring. This symmetry makes all the vibrational modes active. The infrared and Raman data will be analyzed in three parts: aromatic modes, oxazine ring modes, and aliphatic modes. Peak identification for aromatic modes was made by comparing the IR and Raman spectra of model compounds to assignments of substituted benzene derivatives in the text by Varsanyi [13], to assignments of 2,4-dimethylbenzonitrile (24DBN) [14], to assignments of 1,2,4-trimethylbenzene (124TMB) [15], and to assignments of 2,4-dimethylphenol (24DMP) [16]. In addition, the assignments are aided by the vibrational spectra of 3,4-dideutero-3,6-dimethyl-2D-1,3-benzoxazine. For the deuterated system, the peaks with uncertain assignments have a question mark next to their position in Table 2. The spectra of the model compounds are presented in Figs 3–8. The spectra are divided into regions 1700–1300, 1300–900, and 900–500 cm^{-1} for better inspection. Figures 3–5 are infrared spectra of methyl through n-amyl amine plus the deuterated benzoxazine. Figures 6–8 depict the Raman spectra of the molecules described above. Table 2 lists infrared and Raman assignments for the benzoxazines in the fingerprint region.

Aromatic modes

The benzene ring of the benzoxazine molecule has substitutions at the 1, 2 and 4 positions. The positions of the benzene modes should remain almost unaffected despite

the length of the hydrocarbon chain of the amine. Thus, the spectra of the model compounds can be internally compared for stability and relative intensity of the infrared and Raman peaks. The benzene vibrations will be classified as: radial, tangential, or out-of-plane modes.

Radial modes

Radial vibrations are in-plane and normal to the benzene ring. These include C–C–C bending (Wilson number 12, 6a, 6b), ring "breathing" (1), and C–X (7a, 7b, 13) stretching modes. The in-plane carbon modes and the C–X stretching modes are highly coupled, making the carbon in-plane modes substituent sensitive. Vibrational mode 12 is identified by the strong Raman (Fig. 8) and medium intensity IR (Fig. 5) peak at 746 cm^{-1} in all model compounds. This assignment is in good agreement with 24DBN at 750 cm^{-1}, with 24DMP at 767 cm^{-1}, and with 24DMP at 745 cm^{-1}. Mode 6a is located at 587 cm^{-1} while mode 6b can be found below 500 cm^{-1}. Identification of mode 6a is less straightforward than the previous vibration. Only modes 6a and 16a appear in the region from 500 to 600 cm^{-1}. Upon deuteration, peaks at 587 and 546 cm^{-1} shift to 572 and

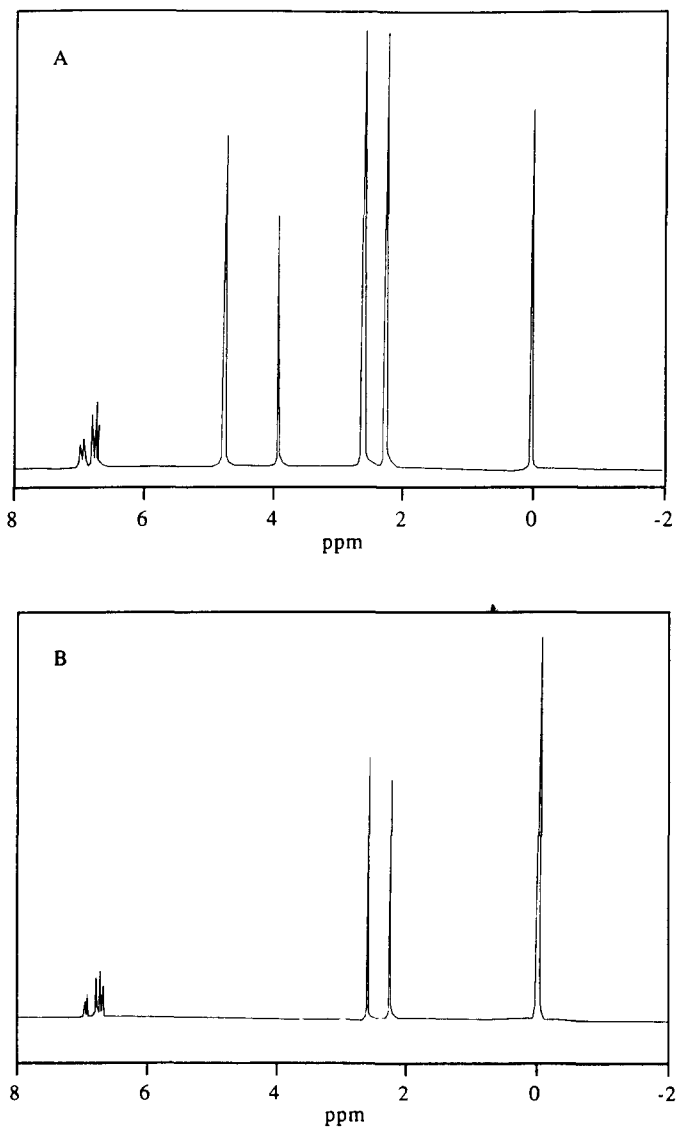

Fig. 1. ^1H NMR spectra of hydrogenated (A) and deuterated (B) 3,6-dimethyl-2H-1,3-benzoxazines.

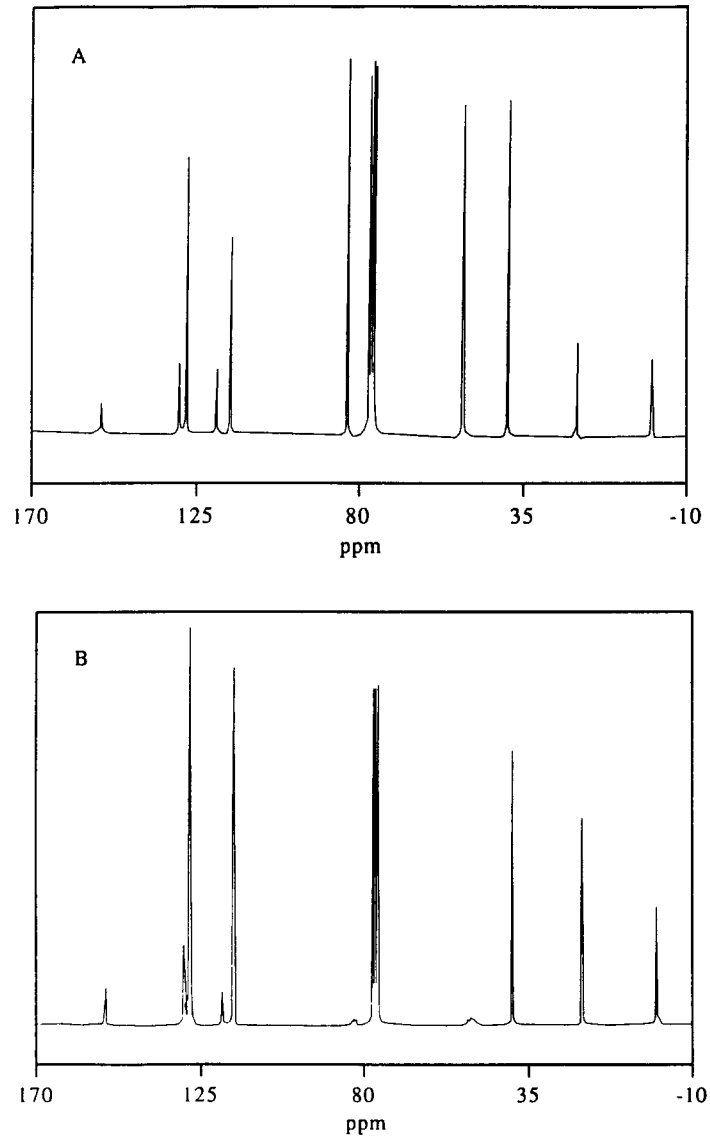

Fig. 2. ^{13}C NMR spectra of hydrogenated (A) and deuterated (B) 3,6-dimethyl-2H-1,3-benzoxazines.

Table 1. NMR assignments of 3,4-dihydro-3,6-dimethyl-2H-1,3-benzoxazine and 3,4-dideutero-3,6-dimethyl-2H-1,3-benzoxazine.

Assignment	Hydrogenated ^{1}H (p.p.m.)	Hydrogenated ^{13}C (p.p.m.)	Deuterated ^{1}H (p.p.m.)	Deuterated ^{13}C (p.p.m.)
C1	4.76	83.7	absent	83.0 (center)
C2	3.91	52.1	absent	51.3 (center)
C3	—	119	—	119
C4	6.79	128	6.78	128
C5	—	130	—	129
C6	6.66, 6.70	128	6.68, 6.72	128
C7	6.91, 6.94	116	6.91, 6.95	116
C8	—	151	—	150
C9	2.25	20.1	2.25	20.6
C10	2.59	39.3	2.56	37.6

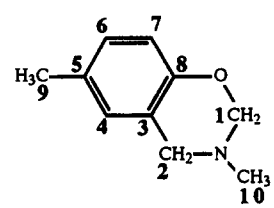

Table 2. Infrared and Raman assignments for model benzoxazines in the fingerprint region.

Methyl/2 CD_2				Methyl/2 CH_2				Ethyl				Propyl				Butyl				Amyl				
IR	Int	Raman	Int	IR	Int	Raman	Int	IR	Int	Raman	Int	IR	Int	Raman	Int	IR	Int	Raman	Int	IR	Int	Raman	Int	Assignment
1616	w	1613	m	1617	w	1614	m	1617	w	1622	m	1617	w	1615	m	1617	w	1623	m	1617	w	1622	m	8b
1585	w	1581	w	1586	w	1590	w	1586	w	1586	w	1587	w	1584	w	1587	w	1592	w	1587	w	1592	w	8a
				1518	w			1520	w			1517	w			1519	w			1521	w			
1494	vs	1492	vw	1500	vs	1497	w	1501	vs	1498	w	1500	vs	1503	w	1501	vs	1499	w	1500	vs	1500		19b
				1488	w			1490	m	1490	w	1489	m			1491	m			1491	m			
								1471	w	1476	w	1471	w	1475	m	1477	w	1475	m	1480	w	1476	w	CH_2 scissoring
1463	w	1459	w	1464	w	1467	m	1468	w			1465	w	1467	s	1466	m	1466	w	1467	w			CH_3 asym. def.
								1460	w	1454	m	1460	w			1457	w			1458	w			CH_2 scissoring
								1452	w			1455	w			1453	w			1452	w			CH_2 scissoring
																1449	w	1449	w	1447	w	1448	s	CH_2 scissoring
1453, 1447	w	1456, 1448	w	1445	m	1444	w																	CH_2 scissoring
						1442	w	1446	w	1445	w	1443	w	1444	w	1444	w			1440	w			CH_2 scissoring
				1421	w	1420	w	1422	w	1422	w	1420	w	1421	w	1419	w	1420	w	1423	w	1420	w	CH_2 scissoring
1417	w	1419	w	1414	w	1414	w	1417	w	1416	w	1417	w	1416	w	1416	w	1414	w	1416	w	1415	w	19a
		1403	w	1393	w	1392	w																	N–CH_3 sym. def.
		1403	w					1389	w	1309	w	1389	w	1390	w	1387	w	1390	w	1388	w	1390	w	(CH_2)–CH_3 sym. def.
1380	w	1379	m	1380	w	1382	m	1380	m	1381	m	1377	m	1381	m	1377	m	1383	m	1377	w	1382	m	ar. CH_3 sym. def.
												1367	w			1365	w			1369	w			CH_2 wag
								1350	w							1353	w							CH_2 wag
				1343	w	1340	w	1341	w	1346	w	1342	w	1340	w	1341	w	1340	w	1341	w	1345	w	CH_2 wag (benzox.)
				1327	m																			
				1321	w			1321	w			1321	m	1321	w	1321	m			1320	m			CH_2 wag (benzox.)
				1304	w			1300	w			1304	w	1300	w	1305	w	1299		1307	w			CH_2 twist
1293	w	1294	w	1293	w	1289	w	1294	w	1297	w	1292	w	1290	w	1292	w	1290	w	1292	w	1295	w	14
				1286	m																			
		1279	w	1278	w											1275	w							
1262	m	1262	w	1265	w	1261	w	1265	w	1270	w	1265	w	1263	w	1265	w	1265	w	1264	w	1265	w	3
				1257	w							1257	w			1251	w			1257	w			CH_2
1243	w	1246	m	1249	w	1248	m	1252	w	1254	m	1248	w	1244	m	1242	w	1248	m	1245	w	1247	w	7a
1231	m			1234	m	1234	m	1237	m	1242	m	1234	s	1230	m	1229	s	1234	m	1225	s	1228	w	13 (C–O–C as. str.)
1226	s	1224	s	1227	vs	1224	w	1226	vs	1231	w	1222	vs	1219	w	1216	m	1220	w	1208	m			13 (C–O–C as. str.)
								1211	m															

				1207	w			1199	w	1196	w	1199	m	1189	w	1192	w	1189	w	1181	w	1182	w	C–N–C asym. str.
				1200	m	1195	w	1192	w	1194	w	1188	w	1184		1183	w	1184	w	1174	w	1170	w	C–N–C asym. str.
1158	w	1158	w	1159	w			1159	w													
												1150	s			1151	m			1149	w			
1136	w	1140	w	1143	m	1141	w	1143	s	1143	w	1143	m	1138	w	1140	m	1143	w	1139	m	1140	w	15
1109	w	1114	w	1133	m	1137	w	1129	w	1124	w	1136	m											C–N–C asym. str.
				1117	m	1121	w	1120	m	1114	w	1118	m	1114	w	1121	m	1120	w	1117	m	1122	w	18b
								1108	w	1106	w	1098	w			1101	w			1101	w	1097	w	C–N–C asym. str.
								1098	m			1084	m	1087	w	1058	w	1093	w	1092	w			C–N–C asym. str.
1081	w	1084	w																					CD_2 scissoring
				1069	w			1076	w	1070	w	1072	w			1073	w	1068	w	1077	w	1077	w	C–N–C asym. str.
1056	w	1060	w					1064	w											1064		1064	w	C–O–C sym. str.
				1048	m	1050	w	1046	w			1047	w	1047	w	1048				1046	w	1052	w	C–O–C sym. str.
								1037	m	1040	w	1041	w			1039	w	1036	w	1038	w	1038	w	C–O–C sym. str.
1023	m	1030	m	1031	w	1035	w					1033	w			1031	w			1033	w			CH_3 rock (aromatic)
																1025	w			1020	w	1024	w	aliphatic
							w	1014	w	1018	w	1018	m	1021	w	1017	w	1018	w					aliphatic
								1005	w			1007	w			1008	w			1011	w			aliphatic
989	w	991	w																					CD_2 wag
		978	w	976	w	980	w	976	w	974	w	979	m	973	w	977	w	980	w	974	w	978	w	CH_3 term. rock
949?	w	940?																						CD_2 wag
			w	959	w							961	w	967	w	965	w							aliphatic
								953	w							949	w							aliphatic
				940	vs	938	w	938	vs	934	w	939	vs			936	vs			938	vs	934	w	10a
924	n			932		930	w							926										
886	w	883	w	912	m	916	w	911	s	915	w	910	s	915	w	913	s	917	w	912	m	918	w	7b
		909?	w	907	m	904	w																	
								902	m					906	w	902	m			904	m			aliphatic
																				898	w	895	w	aliphatic
		889	w					888	w	894	w	888	m	884	w	888	w	890	w	888	w			aliphatic
				873	w	873	w	874	w	870	w	872	w			874	m			871	w			10b
860	w			857	m	860	w			822	m	850	w	846	w	861	w	862	w	856	w	862	w	C–N–C sym str.
										804	w	837	s	837	w			839	w			835	w	C–N–C sym. str.
825?	w	826?	w			830	w																	
816	w			815	s			815	s			815	s	815	w	814	s	811	w	815	s	820	w	11
800?	w																							
												787	w	788	w									

Table 2 (*Continued*)

Methyl/2 CD_2				Methyl/2 CH_2				Ethyl				Propyl				Butyl				Amyl				
IR	Int	Raman	Int	IR	Int	Raman	Int	IR	Int	Raman	Int	IR	Int	Raman	Int	IR	Int	Raman	Int	IR	Int	Raman	Int	Assignment
								770	w			773	w	773	w	770	w	773	w	774	w	775	w	benzox. ring breath.
736	w	734	s	758	w	752	s	756	m	760	m	753	w	758	w	764	w	766	w	759	w	762	w	benzox. ring breath.
722	w	722	vs	744	m	747	vs	744	m	746	vs	745	m	746	vs	745	m	749	vs	745	m	748	vs	12
								737	w			733	w	729	w	730	w			727	w			CH_2 rock
695	w	697	w	710	w	709	w	710	w	712	w	710	w	707	w	710	w	714	w	710	w	712	w	4
								694	w	695	w	692	w	689	w	694	w	696	w	694	w	695	w	CH_2 rock
673	w	674	w	687	w	683	w	688	w	689	w	685	w	685	w	688	w	687	w	688	w			1
												612	w			613	w							
571	w	573	w	587	w	583	w	590	w	590	w	591	w	586	w	591	w	595	w	591	w	594	w	6a
												564	w			565	w							
538	w	540	w	546	w	544	w	547	w	549	w	547	w	544	w	548	w	551	w	548	w	549	w	16a
												538	w			537	w							
														515	w									
										522	w					510	w							
								509	w	510	w	506	w											

539 cm^{-1}. The peak at 587 cm^{-1} is assigned to the in-plane bending mode 6a because this type of mode would be more influenced by deuteration than the out-of-plane skeletal mode, 16a.

Mode 1 is observed at 687 cm^{-1} weakly in the infrared (Fig. 5) and Raman (Fig. 8). This peak was assigned with the aid of 3,4-dideutero-3,6-dimethyl-2D-1,3-benzoxazine. Upon deuteration, this peak shifts from 687 to 674 cm^{-1} in the Raman. The relative intensity between the bands at 747 (mode 12) and 687 cm^{-1} changed from 747 cm^{-1} having the higher intensity before deuteration to 687 cm^{-1} having the higher intensity after deuteration. Strong coupling between modes 12 and 1 can account for this effect. Therefore, the peak at 687 cm^{-1} is assigned to mode 1.

Substituent stretching vibration 7a is identified as a weak peak in the infrared (Fig. 4) and a medium intensity peak in the Raman (Fig. 7) at 1249 cm^{-1}. Sarma assigns mode 7a to 1243 cm^{-1} in 24DBN, while it appears at 1249 cm^{-1} in 124TMB and at 1264 cm^{-1} in 24DMP. Vibrational mode 7b is assigned to the band at 913 cm^{-1} in the spectra. Sarma assigns this mode to a weak band in the IR and a strong, polarized band in the Raman at 935 cm^{-1}. This band appears as a medium intensity peak at 925 cm^{-1} in the infrared spectra of 124TMB and at 932 cm^{-1} in 24DMP. The final C–X stretching mode (13) appears as a variable position peak around 1235 and 1228 cm^{-1} in the infrared and Raman. Mode 13 will be discussed in more detail in the section on benzoxazine ring modes.

Tangential modes

There are three groups of tangential vibrations: carbon–carbon stretching vibrations (8a, 8b, 19a, 19b, 14), in-plane C–X bending vibrations (9a, 9b, 18a), and in-plane C–H bending vibrations (3, 15, 18b). Modes 8a and 8b appear at 1589 and 1620 cm^{-1}, respectively. In the IR and Raman spectra in Figs 3 and 6, these two bands are constant with respect to position and intensity. They also agree well with assignments made by Varsanyi, with 24DBN (1575 and 1620 cm^{-1}), with the spectra of 124TMB (1577 and 1618 cm^{-1}), and with 24DMP (1620 and 1600 cm^{-1}). Carbon stretching mode 19a has a very weak peak in the Raman and a weak intensity peak in the IR at 1415 cm^{-1} in the spectra of the model compounds and appears at 1415 cm^{-1} in the infrared spectrum of 24DMP.

Mode 19b is of strong intensity and constant position in the IR spectra and very weak in the Raman spectra at 1503 cm^{-1}. Mode 19b appears at 1504 in 24DBN, at 1511 in

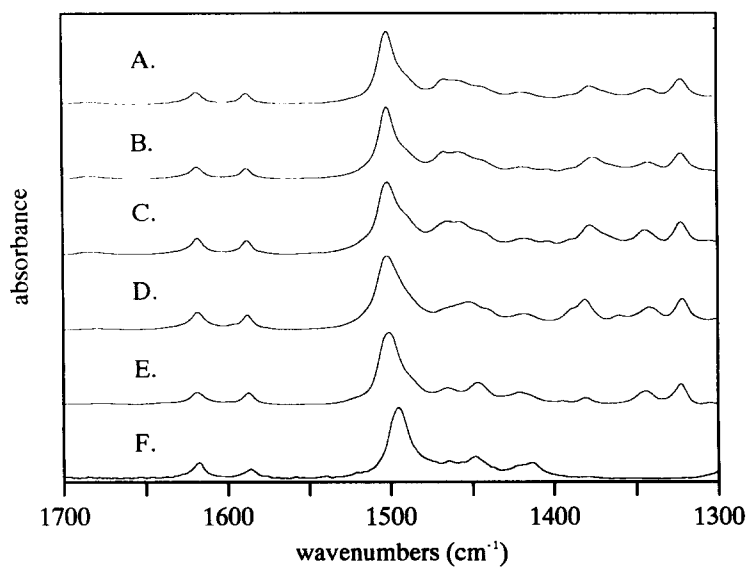

Fig. 3. Infrared spectra of model benzoxazines with various amines: amyl (A), butyl (B), propyl (C), ethyl (D), methyl/2 CH_2 (E), and methyl/2 CD_2 (F).

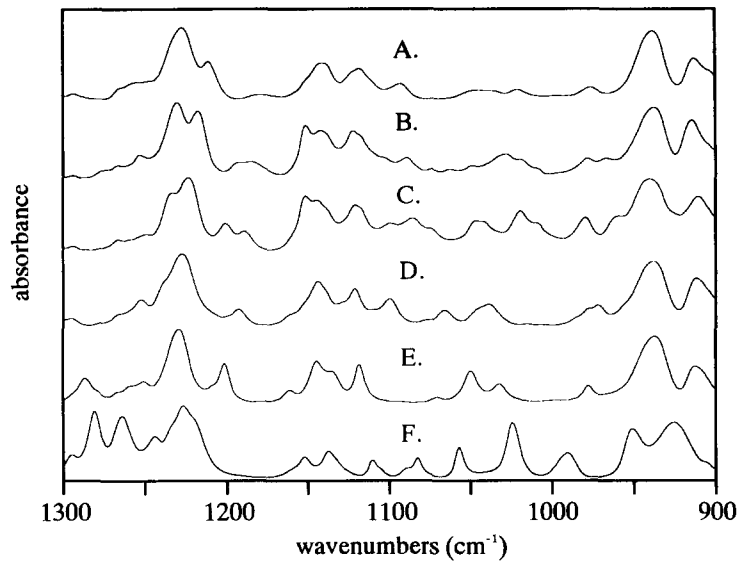

Fig. 4. Infrared spectra of model benzoxazines with various amines: amyl (A), butyl (B), propyl (C), ethyl (D), methyl/2 CH_2 (E), and methyl/2 CD_2 (F).

24DMP, and at 1510 cm^{-1} in the spectrum of 124TMB. Carbon stretching mode 14 appears as a very weak peak in the IR and Raman at 1295 cm^{-1}. In the spectra of 24DBN, 124TMB and 24DMP, this mode is seen at 1291 cm^{-1} for all three molecules. Hydrogen in-plane bending mode 3 is found in the IR (Fig. 4) and Raman (Fig. 7) spectra of the model compound at 1265 cm^{-1}. Mode 15 appears in the benzoxazine spectra at 1141 cm^{-1}, at 1148 cm^{-1} for 24DMP, and at 1156 cm^{-1} for 124TMB. The last C–H in-plane bending mode, 18b, is assigned to the peak at 1120 cm^{-1} for benzoxazines and at 1118, 1110 and 1125 cm^{-1} for 24DBN, 24DMP and 124TMB. C–X in-plane bending modes of 9a, 9b, and 18a would be found in the region 190–390 cm^{-1}.

Out-of-plane modes

The out-of-plane deformations can be skeletal (4, 16a, 16b), C–X (3, 17a, 17b), and C–H (11, 10a, 10b). Mode 4 appears as a constant, weak peak in the spectra of the model

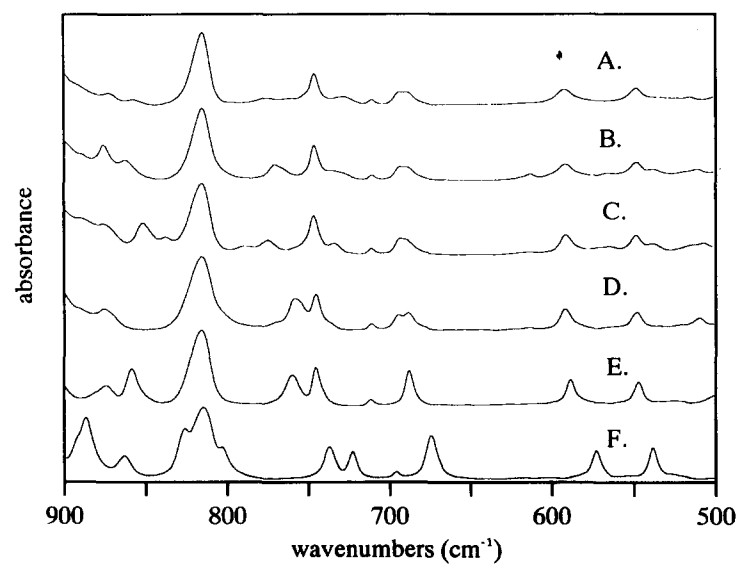

Fig. 5. Infrared spectra of model benzoxazines with various amines: amyl (A), butyl (B), propyl (C), ethyl (D), methyl/2 CH_2 (E), and methyl/2 CD_2 (F).

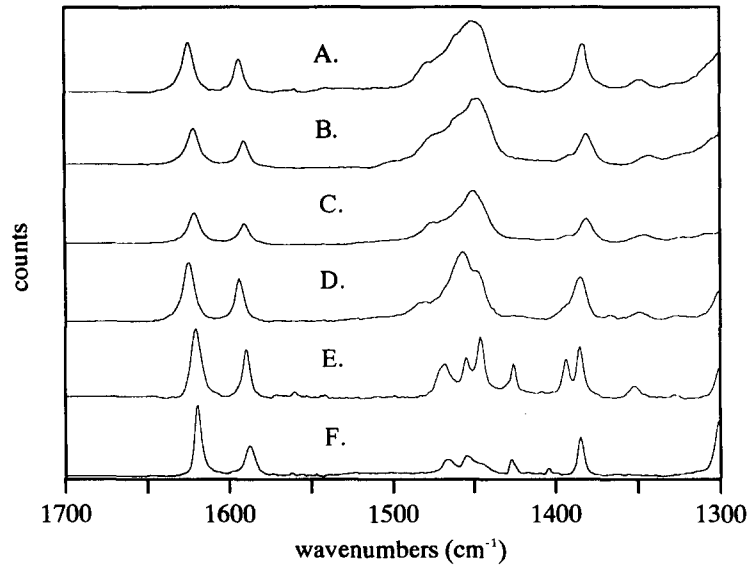

Fig. 6. Raman spectra of model benzoxazines with various amines: amyl (A), butyl (B), propyl (C), ethyl (D), methyl/2 CH_2 (E), and methyl/2 CD_2 (F).

compounds at 710 cm^{-1}, at 716 cm^{-1} for 24DBN, and at 718 cm^{-1} for 24DMP. Mode 16a can be seen at 546 cm^{-1}, while mode 16b appears in the region from 420 to 480 cm^{-1}. The C–X out-of-plane vibrations 5, 17a, and 17b would be found from 190 to 270 cm^{-1}. The first C–H out-of-plane bending mode, 11, is a strong and constant peak in the IR spectra at 816 cm^{-1} and at 827 cm^{-1} for 24DBN. This peak is extremely weak in the Raman spectra. Vibration 10a is strong and constant in the IR at 938 cm^{-1} and appears as a shoulder in the Raman spectra of the model compounds. Mode 10b can be found as a medium intensity peak at 875 cm^{-1} in the infrared spectra of the model compounds, 24DMP and 124TMB. This peak is very weak in the Raman spectra of all these compounds.

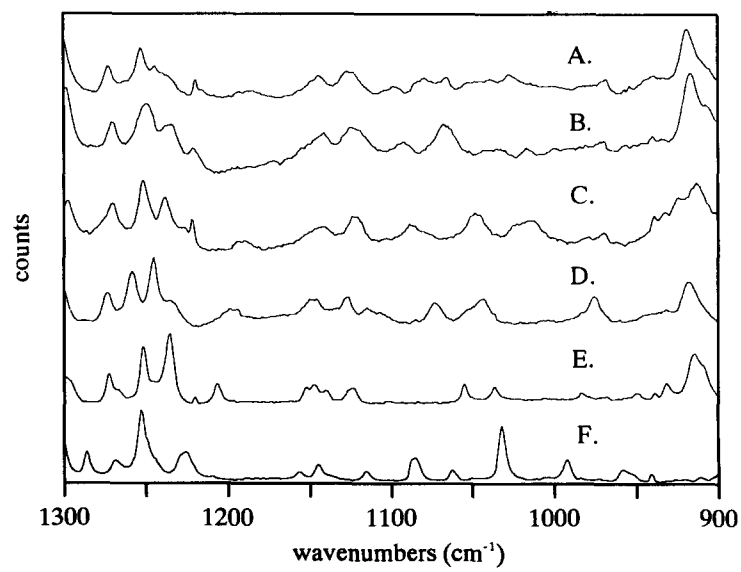

Fig. 7. Raman spectra of model benzoxazines with various amines: amyl (A), butyl (B), propyl (C), ethyl (D), methyl/2 CH_2 (E), and methyl/2 CD_2 (F).

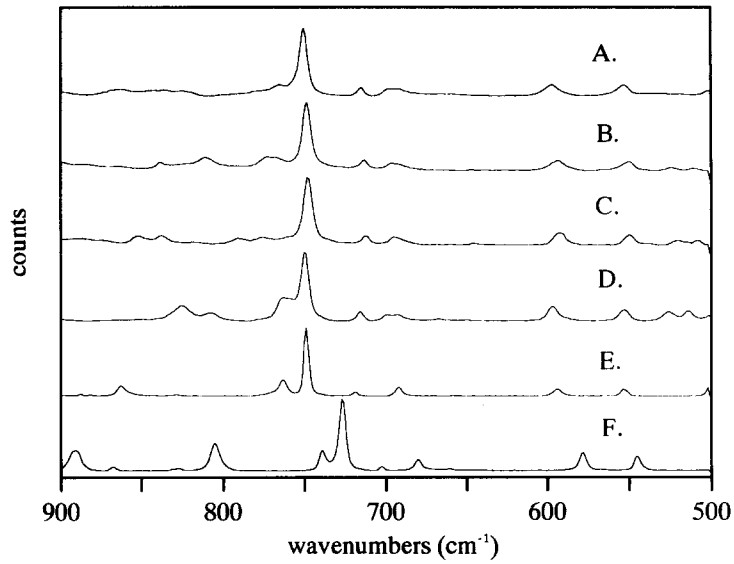

Fig. 8. Raman spectra of model benzoxazines with various amines: amyl (A), butyl (B), propyl (C), ethyl (D), methyl/2 CH_2 (E), and methyl/2 CD_2 (F).

Benzoxazine modes

Unlike the benzene vibrations which are well characterized, oxazine vibrations are not well known. Without normal coordinate analysis, specific vibrations cannot be elucidated. Many oxazine vibrations are heavily coupled to each other and to the benzene ring vibrations. However, the type of vibrations from the oxazine ring that are expected to occur can be seen by inspecting the internal coordinates of a simplified ring. Only the C–O, O–C, C–N, and N–C stretching and radial ring modes (breathing and David's star) should appear above 500 cm^{-1} from analysis of the internal coordinates of the oxazine ring. Although the energy contribution of different vibrations to any one band can only be rigorously analyzed using normal coordinate analysis, assignments will be made based on the bands that appear in regions attributed to specific group frequencies.

The antisymmetric and symmetric C–N–C stretching modes can be found in the regions from 1240 to 1020 cm^{-1} and 830 to 740 cm^{-1}, respectively. It is quite common to find more than one band attributable to the C–N stretching vibrations in each region [17]. The C–N–C modes were assigned by comparing the spectra of triethylamine and tributylamine with the corresponding benzoxazines since they are believed to have C–N peaks similar to tertiary amines. The region from 1200 to 1070 cm^{-1} in the infrared was useful for assigning the antisymmetric C–N–C stretching modes. Prominent bands that can be assigned to primarily antisymmetric C–N–C stretching for the ethyl (butyl) derived benzoxazines occur at 1199, 1192, (1192, 1183) and 1108, 1098 (1101, 1088) cm^{-1}. These bands appear with comparable relative intensity and position in the corresponding amines. Although the C–C stretching modes also appear in this region, these peaks are not assigned to the C–C stretching vibration because the peaks do appear with appreciable intensity in the infrared, which is contradictory to their expected weak intensity. The rest of the series of benzoxazine model compounds were assigned using the spectral characteristics found in the spectra previously discussed. The region that was assigned to C–N–C symmetric stretching can be found from 870 to 800 cm^{-1}. There is a stable peak at 861 cm^{-1} in the infrared and Raman spectra of the three methyl amine based benzoxazines (hydrogenated and deuterated *p*-cresol derived and hydrogenated 2,4-dimethylphenol derived). This peak is assigned to the symmetric C–N–C stretching mode. As the length of the amine increases, a peak around 835 cm^{-1} appears which also bears this assignment. This assignment is consistent with other tertiary amines [18]. The antisymmetric and symmetric C–N–C stretching assignments can be found in Table 2.

The C–O–C antisymmetric and symmetric stretching modes appear in the regions of 1240–1210 and 1040–1020 cm^{-1}, respectively. The assignment of C–O modes of the benzoxazines were based on literature values for which multiple peaks for each vibration have been assigned [19] and on systematic trends in peak position. The antisymmetric C–O–C stretch appears as a split peak at 1234 and 1227 cm^{-1} in the IR and Raman spectra of 3,4-dihydro-3,6-dimethyl-2H-1,3-benzoxazines. With increasing amine length, these bands shift systematically as is seen in Fig. 4. The symmetric C–O–C stretching mode assignments can be found in Table 1. In the infrared spectrum of a similar benzoxazine, the C–O–C antisymmetric and symmetric stretches were assigned to bands at 1222 and 1052 cm^{-1} [9].

The out-of-plane ring modes should appear below 500 cm^{-1}. Of interest in this study is the benzoxazine ring "breathing" and "umbrella" modes, which are similar and essentially involve uniform radial displacement of the atoms in the ring. A benzoxazine radial ring mode appears around 770–760 cm^{-1} and splits upon addition of carbon atoms to the amine. This peak has a relatively weak intensity in the infrared and increases in intensity in the Raman, as a radial ring mode should. The exact mode could not be determined. The ring breathing modes of similar molecules, conformers of isochroman, appear from 682 to 740 cm^{-1} [20].

A verification of the oxazine assignments is done by synthesizing 3,4-dihydro-3,6,8-trimethyl-2H-1,3-benzoxazine. The addition of the methyl group at the 8 position alters the substitution of the benzene ring and thus the benzene modes. The effect on the position of the oxazine bands is minimal. Figure 9 shows good agreement between the peaks attributed to the oxazine ring for the *p*-cresol and 2,4-dimethyl phenol derived benzoxazines. The asterisks designate the bands that remain fixed in position despite modification of substitution of the benzene ring.

Aliphatic modes

The region from 1463 to 1420 cm^{-1} consists of the antisymmetric methyl deformation and methylene scissoring vibrations (Figs 3 and 6). The bands assigned to amine methylene scissoring are at 1470, 1457, 1452, 1440, and 1420 cm^{-1}. The peaks at 1443 and 1423 cm^{-1} are a result of methylene scissoring in the oxazine ring. A peak at 1081 cm^{-1} is attributed to CD_2 scissoring. The methyl antisymmetric deformation appears at 1465 cm^{-1}. The region from 1400 to 1180 cm^{-1} consists of methyl symmetric deformation and methylene wagging and twisting vibrations. The peaks at 1345 and 1320 cm^{-1} are

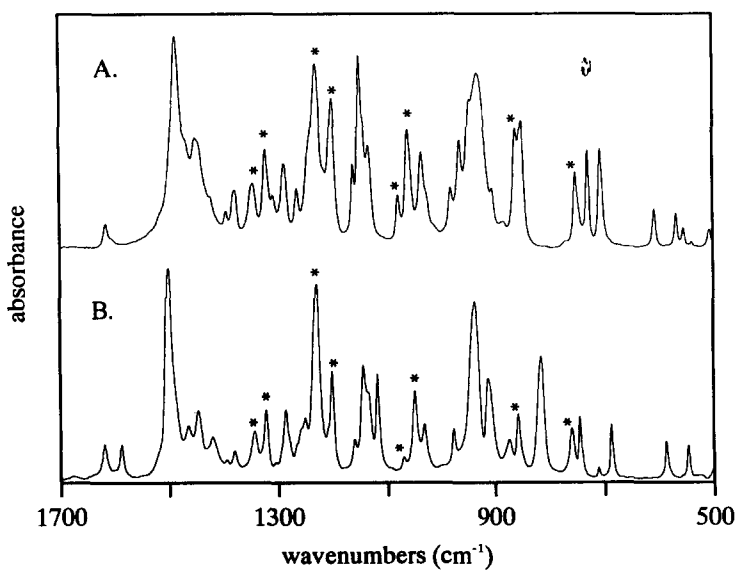

Fig. 9. Infrared spectra of benzoxazines derived from 2,4-dimethylphenol (A) and *p*-cresol (B). The asterisks designate the peaks that remain stable in position despite changing the benzene ring substitution.

unique to the methylene groups in the benzoxazine ring. These peaks disappear upon deuteration of the methylene protons in the ring and shift to 990 and 949 cm^{-1}. The methyl symmetric deformation appears at 1380 cm^{-1} for methyl groups attached to the benzene ring. The methyl symmetric deformation for the methyl amine groups is seen at 1393 cm^{-1} and shifts down to 1390 cm^{-1} for subsequent amines. There are medium to weak bands at 1370, 1350, 1340, 1320, 1305, 1275, and 1251 cm^{-1} assigned to methylene wagging and twisting. The CH_2 twist at 1305 cm^{-1} is assigned to the CH_2 groups in the benzoxazine ring. The shift upon deuteration could not be easily identified. Methyl rocking appears at 1033 cm^{-1} for the methyl group attached to the benzene ring and at about 977 cm^{-1} for the terminal methyl group of the amine. The evolution of intensity of the band around 730 and 696 cm^{-1} (Figs 5 and 8) correlates with an expected increase in the methylene rocking mode with increasing amine length.

There is a region from 1020 to 860 cm^{-1} where many peaks are difficult to assign. Within this region, peaks resulting from C–C stretching and methylene rocking and twisting can be found in the infrared and Raman. Peaks within this region cannot be assigned to a specific vibration but do arise from the presence of the amine since this region becomes more complex as the length of the amine increases. Therefore, those peaks that are unassigned will simply be called aliphatic modes.

REFERENCES

[1] F. W. Holly and A. C. Cope, *J. Am. Chem. Soc.* **66**, 1875 (1944).
[2] W. J. Burke, *J. Am. Chem. Soc.* **71**, 609 (1949).
[3] W. J. Burke, E. L. M. Glennie and C. Weatherbee, *J. Am. Chem. Soc.* **29**, 909 (1964).
[4] W. J. Burke, J. L. Bishop, E. L. Glennie and W. N. Bauer, *J. Org. Chem.* **30**, 3423 (1965).
[5] G. Riess, J. M. Schwob, G. Guth, M. Roche and B. Laude, *Advances in Polymer Synthesis* (Edited by B. M. Culbertson and J. E. McGrath, Plenum, New York (1985).
[6] K. Neuvonen and K. Pihlaja, *J. Chem. Soc. Perkin Trans. II* 461 (1988).
[7] K. Neuvonen and K. Pihlaja, *Mag. Res. Chem.* **28**, 239 (1990).
[8] X. Ning and H. Ishida, Ph.D. Thesis (1991).
[9] D. G. O'Sullivan and P. W. Sadler, *J. Chem. Soc.* 2917 (1957).
[10] Z. Eckstein, P. Gluzinski, W. Hofman and T. Urbanski, *J. Chem. Soc.* 489 (1961).
[11] J. Dunkers and H. Ishida, Ph.D. Thesis (1994).
[12] C. Proponet, B. Laude, M. Ramah and G. Riess, *Spectrochim. Acta* **27A**, 808 (1971).
[13] G. Varsanyi, *Vibrational Spectra of Benzene Derivatives*. Academic Press, New York (1969).
[14] T. V. K. Sarma, *Appl. Spect.* **40**, 933 (1986).
[15] J. H. S. Green, D. J. Harrison and W. Kynaston, *Spectrochim. Acta* **27A**, 808 (1971).
[16] J. H. S. Green, D. J. Harrison and W. Kynaston, *Spectrochim. Acta* **28A**, 33 (1972).
[17] D. Lin-Vien, N. B. Colthup, W. G. Fately and J. G. Grasselli, *The Handbook of Infrared and Raman Characteristics Frequencies of Organic Molecules*. Academic Press, New York (1992).
[18] F. R. Dollish, W. G. Fately and F. F. Bentley, *Characteristic Raman Frequencies of Organic Compounds*, Wiley, New York (1974).
[19] A. R. Katritzky and N. A. Coats, *J. Chem. Soc.* 2062 (1959).
[20] S. K. Freeman, *Appl. Spect.* **24**(1), 42 (1970).